ARTICLE IN PRESS

Available online at www.sciencedirect.com
SCIENCE DIRECT®

ELSEVIER

Chaos, Solitons and Fractals 20 (2004) 427–435

CHAOS
SOLITONS & FRACTALS

www.elsevier.com/locate/chaos

On a possible evidence for Cantorian space–time in cosmic ray astrophysics

Ervin Goldfain

OptiSolve Consulting, 4422 Cleveland Road, Syracuse, NY 13215, USA

Accepted 6 October 2003

Abstract

It is known that invariance under Lorentz transformations is a fundamental principle underlying both relativity and quantum field theory. It has been recently suggested that global Lorentz invariance is only an approximate symmetry of nature that may be broken for subnuclear particles participating in high-energy interactions. In particular, several research groups have argued that violation of Lorentz invariance may provide a satisfactory answer to anomalies reported in the detection of ultrahigh energy cosmic rays (UHECR) and TeV-photon spectra. Since breaking of Lorentz invariance amounts to a manifest violation of relativity, it is highly desirable to search for alternative explanations of these anomalies. Our work suggests a possible solution that complies with relativity and is consistent with the Cantorian geometry of space–time at high-energy scales.
© 2003 Published by Elsevier Ltd.

1. Introduction

It is generally expected that vacuum fluctuations and quantum gravity effects introduce large stochastic perturbations in the space–time geometry at energy scales comparable to the Planck mass [2–9,30–32]. Although this observation has been known since long time, it has not received any serious consideration due to the fact that the Planck mass region is experimentally inaccessible with the current accelerator technology ($M_{\rm Pl} \sim 10^{28}$ eV). The situation has rapidly changed in recent years with the realization that there are cosmic probes that can be affected in their propagation by the fundamental structure of our Universe [8]. These probes are either ultrahigh energy cosmic rays (UHECR) or gamma rays in the TeV range from very far and variable sources. It has been since recognized that cosmology may provide a natural laboratory for testing contemporary theories on ultrahigh energy physics such as loop quantum gravity, quantum foam models of space–time, string/M theories, non-commutative field theories and generalized statistical mechanics (for details see Refs. [26–32] in [1], Refs. [27–33] in [2] and Ref. [3]).

At the same time, there is a growing body of theoretical arguments advocating that vacuum fluctuations at high-energy scales convert the smooth topology of space–time continuum into an infinite dimensional hierarchical Cantor set [30–32]. In this context, it appears that the physics of these cosmic probes may hold valuable clues regarding the underlying geometry of space–time in high-energy interactions.

Detection of UHECR and TeV cosmic rays has revealed a series of discrepancies between theoretical predictions and experimental observations, generically called threshold anomalies. Several research groups have argued that a satisfactory resolution of these anomalies demands giving up the relativistic principle of Lorentz invariance (see Section 4). Since breaking of Lorentz invariance amounts to a manifest violation of relativity, it is highly desirable to search for alternative explanations of these anomalies. Specifically, the dynamic effect of large fluctuations in the interaction

E-mail address: ervingoldfain@hotmail.com (E. Goldfain).

0960-0779/$ - see front matter © 2003 Published by Elsevier Ltd.
doi:10.1016/j.chaos.2003.10.012

energy needs to be accounted for. The paper suggests a possible solution that complies with relativity and is consistent with fractional dynamics and Cantorian geometry of space–time at high-energy scales. Motivation for using fractional dynamics lies in the deep connection between complexity and the fractal topology of phase-space in high-energy interactions. The approach fits the framework opened by fractional extensions of some equations of motion (Poisson [24], Schrodinger [25], Dirac [26] and Klein–Gordon [27]). It is also a consolidation of ideas developed by author in [33,34].

The paper is organized in the following way: Section 2 gives a short description of Lorentz invariance and relativistic mechanics. Review of the UHECR and TeV-photon spectra anomalies is carried out in Section 3. Section 4 deals with specific models for Lorentz invariance violation and their implications. Fractional generalization of the Klein–Gordon equation and Lorentz invariance are detailed in Sections 5 and 6. The energy–momentum conservation corresponding to the fractional kinematics regime is discussed in Section 7. Numerical results and concluding remarks are presented in the last two sections.

2. Lorentz invariance and relativistic mechanics

To make the paper self-contained we introduce below a brief account of Lorentz symmetry. For a more in-depth discussion the reader is referred to [35] and [36].

The invariance of the laws of physics with respect to rotations and with respect to reference frames moving with a constant speed relative to each other is generically called Lorentz invariance. Consider two arbitrary inertial frames (1) and (2) with their coordinate axes oriented in the same direction, one frame moving relative to the other with the velocity V along the x_1-axis. Let $x_4 = ct$, x_j $(j = 1, 2, 3)$ and $x'_4 = ct'$, x'_j represent the set of space–time coordinates of an event recorded in (1) and (2) respectively. The space–time coordinates may be thought of as components of a four-vector. They are related through the Lorentz transformation equations

$$\begin{aligned} x'_1 &= \gamma\left(x_1 - \frac{V}{c}x_4\right) \\ x'_2 &= x_2 \\ x'_3 &= x_3 \\ x'_4 &= \gamma\left(x_4 - \frac{Vx_1}{c}\right) \end{aligned} \tag{1}$$

where c is the light speed in vacuum and

$$\gamma = \frac{1}{\sqrt{1 - \frac{V^2}{c^2}}} \tag{2}$$

Consider a relativistic free particle whose dynamics is specified in terms of energy (E) and momentum $\mathbf{p} = (p_1, p_2, p_3)$. It can be shown that the components of the energy–momentum four-vector (E, p_1, p_2, p_3) transform in the same way as the components of the space–time four-vector. The invariant norms associated with the Lorentz transformation of space–time and energy–momentum four-vectors are given by

$$x^2 - c^2t^2 = x'^2 - c^2t'^2 \tag{3a}$$

$$E^2 - p^2c^2 = E'^2 - p'^2c^2 = m_0^2c^4 \tag{3b}$$

in which m_0 is the rest frame mass of the particle and $x^2 = x_1^2 + x_2^3 + x_3^2$. Relation (3b) is referred to as the relativistic dispersion relation. It is instructive to mention that (3b) is the basis for the derivation of the Klein–Gordon equation of scalar free-field theory [37,38]. By substituting the energy and momentum operators $E \to i\hbar\frac{\partial}{\partial t}$ and $p_j \to -i\hbar\frac{\partial}{\partial x^j}$ in (3b) one obtains

$$\left[\left(\frac{1}{c^2}\frac{\partial^2}{\partial t^2} - \nabla^2\right) + \frac{m_0^2c^2}{\hbar^2}\right]\varphi = 0 \tag{4}$$

in which $\varphi(|x|, t)$ represents the space-symmetric scalar field operator and $\nabla^2 = \frac{\partial^2}{\partial x_1^2} + \frac{\partial^2}{\partial x_2^2} + \frac{\partial^2}{\partial x_3^2}$. Our treatment is developed below in a classical framework where $\varphi(|x|, t)$ is interpreted as an ordinary two-dimensional function and where $\hbar$ and c are set to unity $(\hbar = c = 1)$. To further simplify the formulation and without loss of generality we choose throughout a $1 + 1$ representation of space–time.

3. Review of UHECR and TeV-photon anomalies

We briefly discuss in this section the two anomalies related to the detection of ultrahigh energy cosmic radiation (UHECR) and gamma rays in the TeV range, as described in Refs. [1,4–9,14].

3.1. The UHECR anomaly

This anomaly involves the so-called photopion processes whereby ultrahigh energy protons (p) interact with the cosmic microwave background photons (γ_{CB}) and produce pions (π). The reaction may be symbolically represented as

$$p + \gamma_{CB} \rightarrow p + \pi \tag{5}$$

The expectation is that recording of UHECR protons having energies higher than the standard 5×10^{19} eV threshold (the so-called GZK cutoff) is highly unlikely. Still some ground-based detectors have reported many hundreds of UHECR protons with energies above the GZK threshold and about 20 protons above 10^{20} eV [1,4,14].

3.2. The TeV-photon anomaly

This anomaly refers to high-energy gamma rays (γ) propagating in the intergalactic space and colliding with infrared background photons (γ_{IR}). The result of this interaction is the production of an electron–positron pair according to the process

$$\gamma + \gamma_{IR} \rightarrow e^+ + e^- \tag{6}$$

As in the first anomaly, gamma photons with energies higher than the extinction threshold of 20 TeV should have disappeared from the detection signal. However, observations reported at HEGRA and other ground-based detectors indicate the existence of gamma photons with a spectrum ranging up to 24 TeV, which is above the extinction threshold [1,4,14].

4. Models and implications of Lorentz invariance violation

Various solutions have been proposed to resolve these anomalies. For example, recent work by Kachelrieb et al. suggests a mechanism based on the emergence of new massive hadrons in proton–photon collisions [23]. The prevalent view continues to be that the root cause of anomalies lies in the violation of Lorentz invariance and of the relativistic dispersion relation (3b) [1–22]. Several authors have suggested that Lorentz invariance violation is a manifestation of the short-distance structure of space–time that, in turn, may be accounted for by non-commutative field theories [1,16,17].

Two main models have been put forward. They rely on deformations of the relativistic dispersion relations. Coleman and Glashow have advocated the following extension of the relativistic dispersion relation [7]

$$E_a^2 = \vec{p}^{\,2}_a c_a^2 + m_a^2 c_a^4 \tag{7}$$

where $c_a \neq 1$ is the maximum attainable velocity for the particle labeled by index a. Amelino-Camelia et al. have introduced the dispersion relation [4,14]:

$$E^2 = \vec{p}^{\,2} + m^2 + \frac{|p|^{n+2}}{M_{Pl}^n} \tag{8}$$

in which M_{Pl} is the Planck mass and n a positive exponent.

It can be shown that both (7) and (8) may be mapped into violations of either constancy of light speed in vacuum or the equivalence principle of relativity [21]. In particular, the interval is not invariant to an arbitrary frame change $(x,t) \rightarrow (x',t')$

$$E'^2 - c'^2 p'^2 \neq E^2 - c^2 p^2 \rightarrow x'^2 - c'^2 t'^2 \neq x^2 - c^2 t^2 \quad \text{(Coleman–Glashow)} \tag{9}$$

or, for light-like particles

$$\frac{E'^2}{p'^2} \neq \frac{E^2}{p^2} \neq 1$$
$$\frac{x'^2}{t'^2} \neq \frac{x^2}{t^2} \neq 1 \tag{10}$$

and, respectively

$$\frac{\partial E^2}{\partial(p^2)} \neq 1 \quad \text{(Amelino-Camelia)} \tag{11}$$

By postulating that Lorentz invariance is an approximate symmetry, both models amount to a manifest violation of relativity. It is highly desirable, in this context, to search for alternative explanations of these anomalies. This is the task of the next section where the key ingredients of our approach are introduced and developed.

5. Derivation of the fractional Klein–Gordon equation

We start with the observation that high-energy interactions are characterized by large fluctuations in momenta. In general, strong and steady coupling between fluctuations and the interacting particles under study generates uncontrolled perturbations in the unitary time evolution and drives the transition from order to chaos.

It is known that the chaotic dynamics of Hamiltonian systems is best described as a fractional diffusion process [28,29]. The space–time flow of the probability density function is encoded in a fractional differential equation depending on two non-integer exponents (α, β) responsible for space and time derivatives of the probability distribution function. According to this prescription, the ordinary space and time differentiation operators are extended to

$$\begin{aligned} \frac{\partial}{\partial t} &\rightarrow \frac{\partial^\beta}{\partial t^\beta} \\ \frac{\partial}{\partial |x|} &\rightarrow \frac{\partial^\alpha}{\partial |x|^\alpha} \end{aligned} \tag{12}$$

in which $\partial^\beta/\partial t^\beta$ is the Riemann–Liouville derivative of order $0 < \beta \leqslant 1$ and $\partial^\alpha/\partial|x|^\alpha$ is the Riesz derivative of order $0 < \alpha \leqslant 2$ [28]. Bounding the intervals of the two exponents allows the correct interpretation of the probability density function as a positive scalar. The choice $1 < \beta \leqslant \alpha \leqslant 2$ is also acceptable from this standpoint, as discussed in [28].

Because, in general $\alpha \neq \beta$, differentiation with respect to space and time breaks the dimensional symmetry between these two independent observables. Restoring this symmetry requires introduction of a spatial and temporal mass scale and use of non-dimensional coordinates according to the prescription

$$\begin{aligned} |x^0| &= |x| M_x \\ t^0 &= t M_t \\ \frac{\partial}{\partial t} &\rightarrow M_t^\beta \frac{\partial^\beta}{\partial (t^0)^\beta} \\ \frac{\partial}{\partial |x|} &\rightarrow M_x^\alpha \frac{\partial^\alpha}{\partial |x^0|^\alpha} \end{aligned} \tag{13}$$

The scalar field $\varphi(|x|, t)$ may be naturally interpreted as a probability density function

$$\varphi(|x^0|, t^0) = \phi^2(|x^0|, t^0) \tag{14}$$

where $\phi(|x^0|, t^0)$ represents the probability amplitude of locating the field at $|x^0|$ and t^0.

Under these circumstances, (4) may be extrapolated to

$$\left[\left(M_t^{2\beta} \frac{\partial^{2\beta}}{\partial (t^0)^{2\beta}} - M_x^{2\alpha} \nabla_0^{2\alpha} \right) + m_0^2 \right] \varphi = 0 \tag{15}$$

Furthermore, (15) can be cast into a symmetrical form by using the parameterization

$$\begin{aligned} M_x^\alpha &= M_t^\beta = M \\ m_0^0 &= \frac{m_0}{M} \\ \nabla_0^\alpha &= \frac{\partial^\alpha}{\partial |x^0|^\alpha} \end{aligned} \tag{16}$$

which leads to

$$\left[\left(\frac{\partial^{2\beta}}{\partial(t^0)^{2\beta}} - \nabla_0^{2\alpha}\right) + (m_0^0)^2\right]\varphi = 0 \tag{17}$$

Proceeding by analogy with (4) we perform the generalized operator substitution:

$$\begin{aligned} E^\beta &\to \mathrm{i}\frac{\partial^\beta}{\partial(t^0)^\beta} \\ |p|^\alpha &\to -\mathrm{i}\frac{\partial^\alpha}{\partial|x^0|^\alpha} \end{aligned} \tag{18}$$

which yields in turn the fractional Klein–Gordon equation

$$\left[-E^{2\beta} + |p|^{2\alpha} + (m_0^0)^2\right]\varphi = 0 \tag{19}$$

The correspondence rules (18) are motivated by the following Fourier transform formulas [28,39]:

$$\begin{aligned} &\frac{\partial^{2\beta}}{\partial(t^0)^{2\beta}}\varphi(|x^0|,t^0) \overset{Ft}{\to} (-iE)^{2\beta}\Phi(|p|,E) \\ &\frac{\partial^{2\alpha}}{\partial|x^0|^{2\alpha}}\varphi(|x^0|,t^0) \overset{Fx}{\to} -|p|^{2\alpha}\Phi(|p|,E) \\ &\varphi(|x^0|,t^0) \overset{Fx,t}{\to} \Phi(|p|,E) \end{aligned} \tag{20}$$

where Ft and Fx stand for transform operators with respect to time and space. The resulting dispersion relation

$$E^{2\beta} = |p|^{2\alpha} + (m_0^0)^2 \tag{21}$$

is an obvious generalization of the ordinary relativistic dispersion corresponding to $\alpha = \beta = 1$.

6. Fractional generalization of Lorentz invariance

Consider now the massless relativistic case $m_0^0 = 0$. The fractional Klein–Gordon equation reads

$$\left[\frac{\partial^{2\beta}}{\partial(t^0)^{2\beta}} - \nabla_0^{2\alpha}\right]\varphi = 0 \tag{22}$$

The first order moments of space and time computed from (22) are given by [29]

$$\left\langle |x^0|^{2\alpha}\right\rangle = \text{const.} \times (t^0)^{2\beta} \tag{23}$$

It is seen from (21) and (22) that, in contrast with theories based on Lorentz invariance violation, the principle of constancy of light speed is preserved here since

$$\frac{\partial E^{2\beta}}{\partial(p^{2\alpha})} = 1 \tag{24}$$

and, for any pair of arbitrary frames $(x^0,t^0),(x'^0,t'^0)$

$$\frac{\left\langle |x'^0|^{2\alpha}\right\rangle}{(t'^0)^{2\beta}} = \frac{\left\langle |x^0|^{2\alpha}\right\rangle}{(t^0)^{2\beta}} = \text{const.} \tag{25a}$$

which is a natural generalization of (3a).

It can be also seen from (21) and (23) that the following space–time and energy–momentum substitutions do not alter the form of Lorentz transformations (1) and their norms (3)

$$\begin{aligned} |x_{\mathrm{fr}}^0| &= |x^0|^\alpha \\ t_{\mathrm{fr}}^0 &= (t^0)^\beta \\ |p|_{\mathrm{fr}} &= |p|^\alpha \\ E_{\mathrm{fr}} &= E^\beta \end{aligned} \tag{25b}$$

We wish to elaborate on this point in greater detail. Consider, as before, two inertial frames (1) and (2) and let $X^0_{\rm fr}$ and $T^0_{\rm fr}$ stand for the space–time coordinates locating the origin of frame (2) measured relative to (1). $X^0_{\rm fr}$ and $T^0_{\rm fr}$ are defined according to (25b). The generalized Lorentz transformations for space–time coordinates take the form

$$\begin{aligned} x'^0_{\rm fr} &= \gamma_{\rm fr}(x^0_{\rm fr} - V_{\rm fr}t^0) \\ t'^0_{\rm fr} &= \gamma_{\rm fr}(t^0_{\rm fr} - V_{\rm fr}x^0_{\rm fr}) \end{aligned} \tag{26}$$

where $V_{\rm fr}$ is the equivalent relative fractional velocity between the two frames, that is

$$V_{\rm fr} = \frac{X^0_{\rm fr}}{T^0_{\rm fr}} \tag{27}$$

and

$$\gamma_{\rm fr} = \frac{1}{\sqrt{1 - V^2_{\rm fr}}} \tag{28}$$

In an analogous manner, from (21) and (25b) we obtain

$$E^2_{\rm fr} - p^2_{\rm fr} = E'^2_{\rm fr} - p'^2_{\rm fr} = (m^0_0)^2 \tag{29}$$

There is a straightforward connection between the first two relations in (25b) and the formal definition of the Hausdorff dimension in fractal sets theory. It follows that the two exponents α, β naturally coincide with the fractal dimensions of the underlying Cantorian space–time manifold [28,29]. We shall make use of this property in Section 9.

7. Fractional balance of energy and momentum

Let us now return to the UHECR and TeV-photon spectra anomalies introduced in Section 3. Consider the head on collision between a soft photon having energy ε and momentum $\vec{k}$ and a high-energy particle of energy E_1 and momentum p_1. The process leads to the creation of two particles with energies E_2, E_3 and momenta $\vec{p}_2, \vec{p}_3$, respectively [1,4,14]. The high-energy collision channels corresponding to both anomalies occur on small space–time intervals. For sufficiently small space–time intervals, the irreversible character of fractional diffusion may be neglected. Then the conservation of energy and momentum requires

$$\begin{aligned} E^\beta_1 + \varepsilon^\beta &= E^\beta_2 + E^\beta_3 \\ p^\alpha_1 - k^\alpha &= p^\alpha_2 + p^\alpha_3 \end{aligned} \tag{30}$$

Taking into account that, according to (21), the generalized photon dispersion relation is

$$\varepsilon^\beta = k^\alpha \tag{31}$$

we obtain from (30) and (31)

$$E^\beta_1 + [E^{2\beta}_1 - (m^0_1)^2]^{1/2} = E^\beta_2 + [E^{2\beta}_2 - (m^0_2)^2]^{1/2} + E^\beta_3 + [E^{2\beta}_3 - (m^0_3)^2]^{1/2} \tag{32}$$

The above relation may be specialized for the two paradoxes as described below:

7.1. The UHECR anomaly

In this case

$$\begin{aligned} m^0_1 = m^0_2 &= m^0_{\rm proton} = \frac{940 \times 10^6}{M} \\ m^0_3 &= m^0_\pi = \frac{140 \times 10^6}{M} \\ p_1 &= p_{\rm proton} = \frac{3 \times 10^{20}}{M} \end{aligned} \tag{33}$$

In addition, direct generalization of [1]

$$\frac{p_2}{p_\pi} = \frac{m_{\text{proton}}}{m_\pi} \tag{34a}$$

yields

$$\frac{p_2^\alpha}{p_\pi^\alpha} = \frac{m^0_{\text{proton}}}{m^0_\pi} \tag{34b}$$

Under these circumstances (32) turns into

$$E_1^\beta + [E_1^{2\beta} - (m^0_{\text{proton}})^2]^{1/2} = E_2^\beta + [E_2^{2\beta} - (m^0_{\text{proton}})^2]^{1/2} + E_\pi^\beta + [E_\pi^{2\beta} - (m^0_\pi)^2]^{1/2} \tag{35}$$

in which, from (21)

$$\begin{aligned} p_1^{2\alpha} &= E_1^{2\beta} - (m^0_{\text{proton}})^2 \\ p_\pi^{2\alpha} &= E_\pi^{2\beta} - (m^0_\pi)^2 \end{aligned} \tag{36}$$

7.2. The TeV-photon anomaly

Here we have

$$\begin{aligned} m_1^0 &= m_\gamma^0 = 0 \\ E_2 &= E_3 \\ E_1 &= E_\gamma = \frac{20 \times 10^{12}}{M} \\ m_2^0 &= m_e^0 = \frac{0.511 \times 10^6}{M} \end{aligned} \tag{37}$$

in addition, the following approximation holds [15]

$$E_2 \approx \frac{E_\gamma}{2} \tag{38}$$

(32) becomes accordingly

$$E_\gamma^\beta = \left(\frac{E_\gamma}{2}\right)^\beta + \left[\left(\frac{E_\gamma}{2}\right)^{2\beta} - (m_e^0)^2\right]^{1/2} \tag{39}$$

where

$$p_2^{2\alpha} = p_3^{2\alpha} = \left(\frac{E_\gamma}{2}\right)^{2\beta} - (m_e^0)^2 \tag{40}$$

We seek the set of (α, β) pairs that simultaneously satisfy the system of Eqs. (35), (36), (39) and (40), falling in the range $0 < \beta \leqslant 1$ and $0 < \alpha \leqslant 2$. Since the number of equations exceeds two, we can only obtain solutions in the least square sense. These solutions minimize the error residuals corresponding to (35) and (39) [40]. Details on the least-squares analysis are presented in the next section.

8. Numerical results

Eqs. (35), (36), (39) and (40) were solved in numerical form using the software package MathCad [40]. The mass scale M was chosen to be variable spanning the range from 10^{12} eV ($=1$ TeV) to an energy bound close to the Planck mass, namely 10^{24} eV. The range was divided in six equal increments of 100 eV.

The algorithm employed for running the solver in MathCad requires specification of initial "guess" values for the unknowns α, β. This input provides MathCad a place to start searching for solutions. Five random guess values were assigned to each energy increment. The table and the graph shown below display the average of the five solutions found for each mass scale as functions of $\log M$.

Data table		
$\log M$	Alpha	Beta
12	0.236	0.155
14	0.210	0.139
16	0.164	0.238
18	0.116	0.184
20	0.185	0.197
22	0.201	0.739
24	0.249	0.821

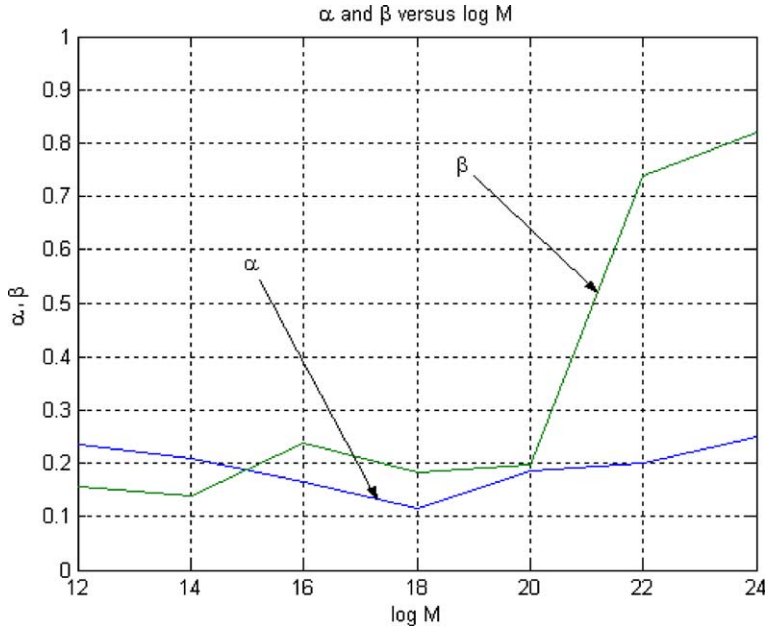

9. Discussion and concluding remarks

Examination of the above data suggests that fractional kinematics contained in (21), (30) and (32) leads to a fairly flat graph for α and a monotonical graph for β above $M \approx 10^{20}$ eV. It is found that α is reasonably close to $\phi^3 = 0.236067977$ where $\phi = \frac{\sqrt{5}-1}{2}$ is the golden mean, which plays a distinctive role in the KAM theory of transition to chaos and in the $E^{(\infty)}$ model of El Naschie. ϕ^3 is the difference between the expectation value for the Hausdorff dimension of space–time in the $E^{(\infty)}$ model and $D = 4$, the dimension of space–time at low energy scales [30–32]. Therefore

$$\alpha \approx \phi^3 = < d_c > -D \tag{41}$$

We caution that these findings are preliminary and require further independent confirmation. In particular, as pointed out in (1), the experimental data needs to be refined and consolidated. Computations presented in this work have used the highest energy values for UHECR and TeV-photons available from current data.

References

[1] Chen S-X, Yang Z-Y. Available from: arxiv:hep-th/0211237.
[2] Bartolami O. Available from: arxiv:hep-ph/0301191.

[3] Beck C. Physica 2002;305A:209, Available from: arxiv: cond-mat/0110007 and arxiv: cond-mat/0301354.
[4] Amelino-Camelia G, Piran T. Phys Rev D 2001;64:036005.
[5] Carmona JM, et al. Available from: arxiv:hep-th/0207158.
[6] Mestres LG. Available from: arxiv: physics/9704017.
[7] Coleman S, Glashow SL. Phys Rev D 1999;59:116008.
[8] Aloisio R et al. Phys Rev D 2000;62:053010, Available from: arxiv: astro-ph/0210402.
[9] Bertolami O, Carvalho CS. Phys Rev D 2002;61:103002.
[10] Sato H. Available from: arxiv: astro-ph/0005218 and arxiv: astro-ph/0304100.
[11] Kifune T. Astrophys J 1999;518:L21.
[12] Kluzniak W. Available from: arxiv: astro-ph/9905308.
[13] Protheroe RJ, Meyer H. Phys Lett B 2000;493:1.
[14] Amelino-Camelia G. Int J Mod Phys D 2002;11:35.
[15] Stecker FW. Available from: arxiv: astro-ph/0304527;
Stecker FW, Glashow SL. Astropart Phys 2001;16:97.
[16] Carmona JM, Cortes JL. Available from: arxiv:hep-th/0207158;
Phys Rev D 2001;65:025006.
[17] Calmet X, Wohlgenannt. Phys Rev D 2003;68:025016.
[18] Jacobson T, et al. Available from: arxiv:gr-qc/0303001.
[19] Grishkan YuS, et al. Available from: arxiv: astro-ph/0203279.
[20] Biermann PL. In: AIP Conference Proceedings, International Workshop Metepec, Puebla, Mexico, 2000.
[21] Halprin A, Kim HB. Available from: arxiv:hep-ph/9905301.
[22] Gonzalez-Mestres L. Available from: www.icrc.1999.utah.edu/~icrc1999/root/vol1/h1_3_16.pdf.
[23] Kachelrieb M et al. Phys Rev D 2003;68:043005.
[24] Derrienic M, Lin M. Israel J Math 2001;123:93–130.
[25] Laskin N. Available from: arxiv:quant-ph/0206098.
[26] Raspini A. Fizika B (Zagreb) 2000;9(2):49–54.
[27] Barci DG, et al. Available from: arxiv:hep-th/9606183.
[28] Zaslavsky GM. Physica D 1994;76:110;
Saichev AI, Zaslavsky GM. Chaos 1997;7(4):753.
[29] Zaslavsky GM, Edelman M. Available from: arxiv.org/PS_cache/nlin/pdf/0112/0112033.pdf.
[30] El Naschie M. Chaos, Solitons & Fractals 2003;17:631–8.
[31] El Naschie M. Chaos, Solitons & Fractals 2003;17:797–807.
[32] El Naschie M. Chaos, Solitons & Fractals 2003;18:401–20.
[33] Goldfain E. Chaos, Solitons & Fractals 2003;17:811–8.
[34] Goldfain E. On the relationship between Hamiltonian chaos and classical gravity. Chaos, Solitons & Fractals 2003;20:187–94.
[35] Barut AO. Electrodynamics and classical theory of fields and particles. New York: Dover; 1980.
[36] Corben HC, Stehle P. Classical mechanics. New York: Dover; 1977.
[37] Messiah A. Quantum mechanics. New York: Dover; 1999.
[38] Hatfield B. Quantum field theory of point particles and strings. Westview Press; 1992.
[39] Podlubny I. Fractional differential equations. Academic Press; 1999.
[40] MathCad is a mathematics software package from MathSoft Inc. 101 Main Street, Cambridge, MA 02142, USA.